

# Revealing complex relaxation behavior of monohydroxy alcohols in a series of octanol isomers

Cite as: J. Chem. Phys. 159, 054501 (2023); doi: 10.1063/5.0160894

Submitted: 6 June 2023 • Accepted: 3 July 2023 •

Published Online: 1 August 2023



View Online



Export Citation



CrossMark

Till Böhmer,<sup>1,a)</sup>  Timo Richter,<sup>1</sup>  Jan Philipp Gabriel,<sup>2</sup>  Rolf Zeißler,<sup>1</sup>  Peter Weigl,<sup>1,3</sup>  Florian Pabst,<sup>4</sup>  and Thomas Blochowicz<sup>1</sup> 

## AFFILIATIONS

<sup>1</sup>Institute for Condensed Matter Physics, Technical University of Darmstadt, 64289 Darmstadt, Germany

<sup>2</sup>Glass and Time, IMFUFA, Department of Science and Environment, Roskilde University, Roskilde, Denmark

<sup>3</sup>Institute for Applied Physics, Technical University of Darmstadt, 64289 Darmstadt, Germany

<sup>4</sup>Laboratory of Polymers and Soft Matter Dynamics, Université Libre de Bruxelles, Brussels, Belgium

<sup>a)</sup> Author to whom correspondence should be addressed: [till.boehmer@pkm.tu-darmstadt.de](mailto:till.boehmer@pkm.tu-darmstadt.de)

## ABSTRACT

We investigate the reorientation dynamics of four octanol isomers with very different characteristics regarding the formation of hydrogen-bonded structures by means of photon-correlation spectroscopy (PCS) and broadband dielectric spectroscopy. PCS is largely insensitive to orientational cross-correlations and straightforwardly probes the  $\alpha$ -process dynamics, thus allowing us to disentangle the complex dielectric relaxation spectra. The analysis reveals an additional dielectric relaxation contribution on time scales between the structural  $\alpha$ -process and the Debye process. In line with nuclear magnetic resonance results from the literature and recent findings from rheology experiments, we attribute this intermediate contribution to the dielectric signature of the O–H bond reorientation. Due to being incorporated into hydrogen-bonded suprastructures, the O–H bond dynamically decouples from the rest of the molecule. The relative relaxation strength of the resulting intermediate contribution depends on the respective position of the hydroxy group within the molecule and seems to vanish at sufficiently high temperatures, i.e., exactly when the overall tendency to form hydrogen bonded structures decreases. Furthermore, the fact that different octanol isomers share the same dipole density allows us to perform an in-depth analysis of how dipolar cross-correlations appear in dielectric loss spectra. We find that dipolar cross-correlations are not solely manifested by the presence of the slow Debye process but also scale the relaxation strength of the self-correlation contribution depending on the Kirkwood factor.

© 2023 Author(s). All article content, except where otherwise noted, is licensed under a Creative Commons Attribution (CC BY) license (<http://creativecommons.org/licenses/by/4.0/>). <https://doi.org/10.1063/5.0160894>

## INTRODUCTION

Monohydroxy alcohols (MAs) have long been popular substances studied to gain a deeper understanding of molecular dynamics in hydrogen bond (H-bond) forming liquids. To study the different relaxation processes in supercooled MAs, mostly broadband dielectric spectroscopy (BDS) has been applied, probing the reorientation dynamics of permanent electric dipole moments. In prototypical supercooled liquids, the slowest relaxation process observed in the dielectric spectrum is the structural relaxation, or  $\alpha$ -process, interpreted as the collective reorientation of molecules coupled to viscosity. By contrast, the dielectric spectra of MAs typ-

ically contain an additional process at even longer timescales that often accounts for the majority of the dielectric relaxation strength.<sup>1</sup> Its single-exponential shape, atypical for the heterogeneous dynamics in supercooled liquids, leads to its designation as the *Debye process*.<sup>2</sup> While the exact microscopic origin of the Debye process is not fully understood, its connection to hydrogen-bonded structures has been established early, resulting in numerous explanatory models.<sup>2–8</sup> Among the more successful ones is the transient-chain model, based on findings from nuclear magnetic resonance (NMR) spectroscopy,<sup>9</sup> where alcohol molecules form chain-like suprastructures via hydrogen bonding, with the molecular dipole moments of the C–O–H moiety adding up along the chain, leading to large

effective end-to-end dipole moments. The origin of the Debye process is considered to be the reorientation of these structures, which proceeds via the attachment and detachment of alcohol molecules. It was suggested that by comparing the relaxation strengths of the Debye- and  $\alpha$ -processes, it is possible to estimate the average number of molecules bound into a single chain in analogy with Rouse dynamics in polymers.<sup>9</sup> The transient-chain model explains many experimental observations; however, it is vague in its conclusions about the exact geometry of the structures that occur and about the dynamics of single molecules within suprastructures.

In general, the types of suprastructures that are predominantly formed depend strongly on the exact molecular architecture of the MA.<sup>10–13</sup> While the molecules of primary MAs such as 1-octanol tend to form linear chains,<sup>11,14</sup> the situation is different if the hydroxy group is located closer to the center of the molecule.<sup>10</sup> The larger steric hindrance with respect to the hydroxy group makes the formation of chain-like structures energetically disfavored compared to primary MAs, resulting in shorter chain-like or even ring-like structures with smaller effective end-to-end dipole moments. Following the transient chain model, the relaxation strength of the Debye process should, therefore, decrease with increasing steric hindrance in the vicinity of the hydroxy group.

The most famous example and model system for the influence of molecular architecture is the series of octanol isomers of the form  $n$ -methyl-3-heptanol, which has been studied in detail for several decades.<sup>15–24</sup> By shifting the methyl group closer to the hydroxy group, the overall dielectric relaxation strength  $\Delta\epsilon$  strongly decreases.<sup>15–17</sup> The latter goes along with a reduction in the relaxation strength of the Debye process.<sup>21</sup> These findings are explained by the existence of ring-like suprastructures in alcohols with large steric hindrance at the hydroxy group, which can be verified by calculating the Kirkwood correlation factor  $g_K$  from the dielectric data.  $g_K$  quantifies the average strength of orientational cross-correlations between adjacent dipole moments, where  $g_K > 1$  indicates predominantly parallel orientation, as would be the case in linear chains, while  $g_K < 1$  indicates predominantly anti-parallel orientation, as expected in ring-like structures.<sup>25–27</sup> Figure 1(a) displays  $g_K$  determined in this work as a function of temperature for four octanol isomers, whose corresponding structural formulas are shown in Fig. 1(b). The values of  $g_K$  were calculated as follows:

$$g_K = \frac{9k_B\epsilon_0MT}{\rho N_A\mu^2} \frac{(\epsilon_s - \epsilon_\infty)(2\epsilon_s + \epsilon_\infty)}{\epsilon_s(\epsilon_\infty + 2)^2}, \quad (1)$$

where  $\epsilon_s$  and  $\epsilon_\infty$  are the zero and high frequency limits of the dielectric permittivity,  $T$  is the temperature,  $M$  is the molar mass,  $\rho$  is the density, and  $\mu$  is the gas-phase molecular dipole moment.<sup>25</sup> Here, we chose  $\epsilon_\infty = 1.05n^2$ , where  $n$  is the refractive index, and  $\mu = 1.68$  D, as proposed earlier by Dannhauser.<sup>16</sup> While for 3-methyl-3-heptanol and 4-methyl-3-heptanol very low Kirkwood correlation factors below unity are observed,  $g_K > 1$  is found for the primary octanol isomer 2-ethyl-1-hexanol. An intermediate role is taken by 5-methyl-3-heptanol, which features a transition from  $g_K < 1$  to  $g_K > 1$  as a function of temperature that can be interpreted as a transition from ring-like to chain-like structures being favored, while both ring-like and chain-like structures coexist over a certain temperature range.<sup>21,28</sup> This coexistence of both structures also explains

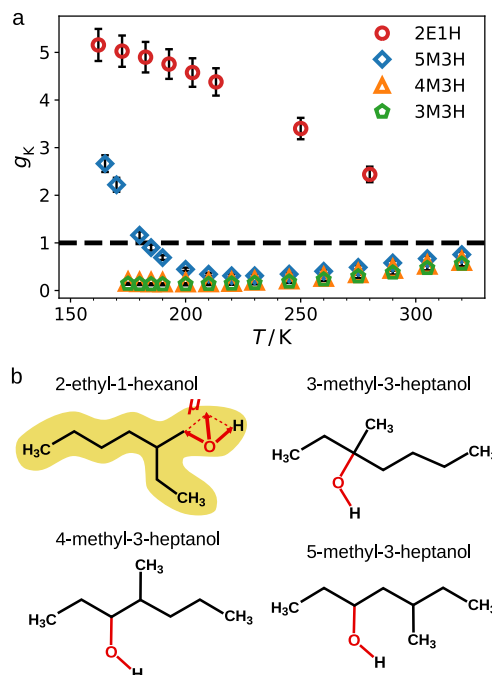


**FIG. 1.** Overview of the four investigated octanol isomers: (a) Kirkwood correlation factors at different temperatures. (b) Molecular structures and a schematic illustration of which molecular moieties are probed by the different experimental techniques. PCS probes the reorientation of the optical anisotropy tensor (yellow), whereas BDS probes the reorientation of the molecular dipole moment  $\mu$  (red). In MAs, the orientation of the latter depends on the orientations of the C–O and the O–H bonds.

the occurrence of a Debye-like relaxation in substances with the predominantly antiparallel ordering of dipoles and  $g_K < 1$ .

Usually, the dielectric loss spectra of MAs can be described by the sum of the slow Debye process and the  $\alpha$ -process, plus additional secondary relaxation processes at high frequencies. By contrast, the recent work by Arrese-Igor *et al.*<sup>29,30</sup> drew attention to the fact that for some alcohols, such as 2-ethyl-1-hexanol, this description is insufficient, with the fit underestimating the relaxation strength in the intermediate region between the Debye- and  $\alpha$ -processes. Since the complex viscosity representation of shear data shows an additional relaxation in exactly this intermediate region, it was concluded that this *intermediate process* might also appear in the dielectric spectrum. One possible interpretation is that the intermediate process results from the reorientation of hydroxy groups as they attach and detach from hydrogen-bonded aggregates.<sup>29</sup> This interpretation is consistent with the fact that the reorientation of hydroxy groups probed by NMR spectroscopy has been shown to be faster than the Debye relaxation but slower than the  $\alpha$ -process, e.g., in 2-ethyl-1-butanol<sup>31</sup> or  $n$ -butanol.<sup>9</sup> The challenge arising when searching for the dielectric signature of such an intermediate relaxation is to identify weak relaxation contributions in relaxation spectra dominated by the strong Debye process. In addition, as BDS spectra always include several overlapping relaxation contributions, the  $\alpha$ -process

and additional intermediate relaxations usually have to be determined by curve fitting the spectra and, thus, the results strongly depend on the applied fit model.

To deal with this issue, we use depolarized photon correlation spectroscopy (PCS), which has been proven to be rather insensitive toward molecular cross-correlations and, thus, usually does not probe the Debye process found in BDS but only the  $\alpha$ - and additional secondary relaxations, i.e., the self-part of reorientational dynamics.<sup>32,33</sup> Only on some occasions was a slow contribution observed in the PCS spectra of MAs, which, however, is significantly weaker than the  $\alpha$ -process.<sup>34</sup> A systematic comparison of BDS and PCS data of different molecular glass formers, including several MAs, revealed that the time constant and spectral shape of the  $\alpha$ -process coincide between both techniques.<sup>35</sup> Consequently, PCS serves as a tool to precisely determine the time constant and spectral shape of the  $\alpha$ -process in the mentioned octanol isomers.

While both techniques examine molecular reorientation, it is important to consider that there are certain differences regarding what molecular aspect is probed. Namely, the reorientation of molecular dipole moments in BDS and the reorientation of the molecular optical anisotropy tensor in PCS. In the specific case of long-chained MAs such as octanol isomers, the consequence is that BDS and PCS are sensitive to the reorientation of very different portions of the molecules: As illustrated in Fig. 1(b) for 2-ethyl-1-hexanol, the entire molecule, including the carbon-backbone, contributes to the optical anisotropy depicted in yellow. By contrast, the geometry of the C–O–H moiety almost entirely determines the direction of the molecular dipole moment (depicted in red). Therefore, PCS mostly probes the reorientation of the carbon-backbone, while BDS specifically probes the dynamics of the C–O–H moiety. Additionally, one could expect  $\tau_{\text{BDS}} = 3\tau_{\text{PCS}}$  to hold for the respective relaxation times probed in both techniques in the case of isotropic and diffusive rotation. The reason for this is that the respective orientational correlation functions are related to Legendre polynomials of different orders, i.e., order  $\ell = 1$  for BDS and  $\ell = 2$  for PCS.<sup>36</sup> While it is certainly reasonable to consider this as a possible relation between both time constants, the factor of three is usually not confirmed in experiments on supercooled liquids and was also not found in mathematical models that consider more realistic motional mechanisms.<sup>37</sup>

In this study, we utilize the mentioned differences between both experimental techniques by performing a joint analysis of BDS and PCS data. PCS results show that for all studied octanol isomers, the  $\alpha$ -process dynamics of the entire molecule are fairly simple and resemble the behavior of many other supercooled liquids. This information allows us to further disentangle the different contributions to the BDS spectra and to reveal that dipolar relaxation in these MAs can only be understood considering a remarkably complex superposition of self- and cross-correlational dynamics on different timescales. We approach explaining the origin of this behavior by combining our own results with results from site-specific NMR experiments from the literature.

## EXPERIMENTAL DETAILS

Samples of 2-ethyl-1-hexanol (2E1H, Sigma–Aldrich, 99%), 5-methyl-3-heptanol (5M3H, TCI Chemicals, 98%), 4-methyl-3-heptanol (4M3H, Alfa Aesar, 99%), and 3-methyl-3-heptanol

(3M3H, TCI Chemicals, 98%) were purchased and filtered into PCS sample-cells using 200 nm hydrophobic syringe filters. The dielectric samples were prepared without further purification. BDS measurements were performed using a Novocontrol Alpha-N High Resolution Dielectric Analyzer in combination with a home-built time domain setup (details in Ref. 38). PCS measurements were performed in depolarized/vertical–horizontal (VH) geometry under a scattering angle of 90° in a setup described earlier in detail.<sup>39–41</sup> Generally, a broad temperature range is covered, except for 5M3H, where only temperatures below 170 K could be measured due to the turbidity of the sample. At low temperatures, turbidity could be avoided by rapidly cooling from high temperatures to a temperature just below  $T_g$  with cooling rates  $>6$  K/min. At these temperatures, the sample stayed transparent for  $>24$  h.

The autocorrelation function  $g_2(t) = \langle I(t)I(0) \rangle / \langle I \rangle^2$  of the scattered light intensity  $I$  probed in PCS is related to the electric field autocorrelation function  $g_1(t) = \langle E^*(t)E(0) \rangle / \langle |E| \rangle^2$  via the Siegert relation for partially heterodyne scattering, as explained in more detail earlier.<sup>39</sup> In order to allow for a direct comparison to BDS data, we calculate the imaginary part of the generalized complex light-scattering susceptibility  $\chi''(\omega)$  from  $g_1(t)$  via<sup>42</sup>

$$\chi''(\omega) = \omega \int_0^\infty g_1(t) \cos(\omega t) dt, \quad (2)$$

numerically implemented by using the Filon algorithm.<sup>43</sup> We note that the light-scattering susceptibility  $\chi''$  should not be confused with the dielectric susceptibility. To allow for a precise comparison between results from PCS and BDS, temperature calibration was performed carefully, resulting in an overall accuracy of at most  $\pm 0.5$  K between the different setups. For 4M3H, additional high-temperature measurements were performed at 280 K. Light-scattering data were obtained using a Tandem Fabry–Perot interferometer (TFPI) by JRS Scientific Instruments in depolarized backscattering geometry.<sup>44</sup> To obtain dielectric data in a comparable frequency range, we combined data from a RF impedance analyzer E4991A by Agilent Scientific Instruments (70 MHz–1 GHz)<sup>44</sup> and a PNA-L Network Analyzer 5230c from Agilent equipped with the slim form probe (600 MHz–3 GHz).

## RESULTS

We begin by analyzing the spectral shape of the  $\alpha$ -process observed in PCS for the different octanol isomers in Fig. 2. For each substance,  $\chi''$  at a temperature just above the respective  $T_g$  is plotted as a function of the reduced frequency  $\tau_{\text{peak}}\nu$ . The shape of the  $\alpha$ -process for all octanol isomers almost perfectly coincides up to frequencies where secondary relaxations appear. This common shape is well described by the *generic shape* of the  $\alpha$ -process, which has recently been observed in PCS for a broad range of different MAs and other supercooled liquids.<sup>35</sup>

In Fig. 3, we compare  $\chi''$  to the dielectric loss  $\epsilon''$  measured at the same temperatures. The shape of  $\epsilon''$  varies strongly between the different MAs, in line with the broad range of observed  $g_K$  values: For chain-forming MAs (2E1H and, in addition, 5M3H at the shown temperature), spectra are dominated by a narrow Debye peak featuring a distinct hump at higher frequencies, which previously has been interpreted as the  $\alpha$ -process. By contrast, ring-forming MAs (4M3H and 3M3H) display a broad plateau-like multi-modal peak,

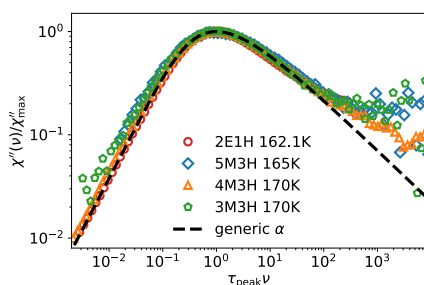


**FIG. 2.**  $\alpha$ -process of all four investigated octanol isomers as probed by PCS and normalized to the peak maximum frequency for comparison. Temperatures are chosen such that the respective peak-maximum frequencies roughly coincide. The dashed line represents a susceptibility function based on a generalized gamma distribution<sup>45</sup> of relaxation times with parameters  $\alpha = 2$  and  $\beta = 0.5$  representing the generic  $\alpha$ -relaxation shape that was observed by PCS in a broad range of different supercooled liquids.<sup>35</sup>

which has been interpreted as a superposition of a Debye-like and the  $\alpha$ -process with comparable relaxation strength.

For a qualitative comparison between  $\epsilon''$  and  $\chi''$ , the respective peak maximum frequencies of the latter are indicated as black lines. For the chain-forming MAs, the peak maximum frequency of  $\chi''$  matches the high-frequency hump in  $\epsilon''$ , suggesting a rough coincidence of the respective  $\alpha$ -processes in both techniques. For ring-forming MAs, the main peak in  $\chi''$  is observed at approximately a factor of ten higher frequencies than the broad plateau observed in  $\epsilon''$ . Additionally, the insets in Fig. 3 display a comparison of how the  $\beta$ -processes are probed by the two techniques. In all cases, the peak maximum frequencies and approximately the shape coincide between the techniques. In 4M3H, a high-frequency excess wing instead of a  $\beta$ -process is observed in both techniques; therefore, no low temperature data of 4M3H are included in Fig. 3.

### Combined spectral analysis of $\epsilon''$ and $\chi''$

As discussed in detail above, BDS and PCS are sensitive to different aspects of molecular dynamics in octanol isomers. Therefore, considering the findings in Fig. 2, we can conclude that the  $\alpha$ -process dynamics of the entire octanol molecules, probed in PCS, are simple, unimodal, and represent the typical behavior in supercooled liquids.<sup>35</sup> In contrast, the dipolar relaxation, mostly coupling to the C–O–H moiety of the molecules, contains contributions over a broad frequency range and has a complex shape. In previous studies of other MAs,<sup>32–34</sup> e.g., 1-propanol, it was found that dielectric loss spectra are well described as a superposition of the  $\alpha$ -process as probed in PCS and a Debye process, reflecting dipolar cross-correlations due to the formation of suprastructures. Quantitatively, this corresponds to  $\epsilon''$  being well described by

$$\epsilon''(\nu) = \Delta\epsilon_D \cdot \text{Im}\left(\frac{1}{1 + i(2\pi\nu)\tau_D}\right) + \Delta\epsilon_{\alpha\beta} \cdot \chi''(\nu), \quad (3)$$

i.e., the weighted sum of the fit to  $\chi''$  and a Debye function with respective relaxation strengths  $\Delta\epsilon_{\alpha\beta}$  and  $\Delta\epsilon_D$ . The underlying assumption of this approach is that the  $\alpha$ - and  $\beta$ -processes of the entire molecule and the C–O–H moiety carrying the dipole moment

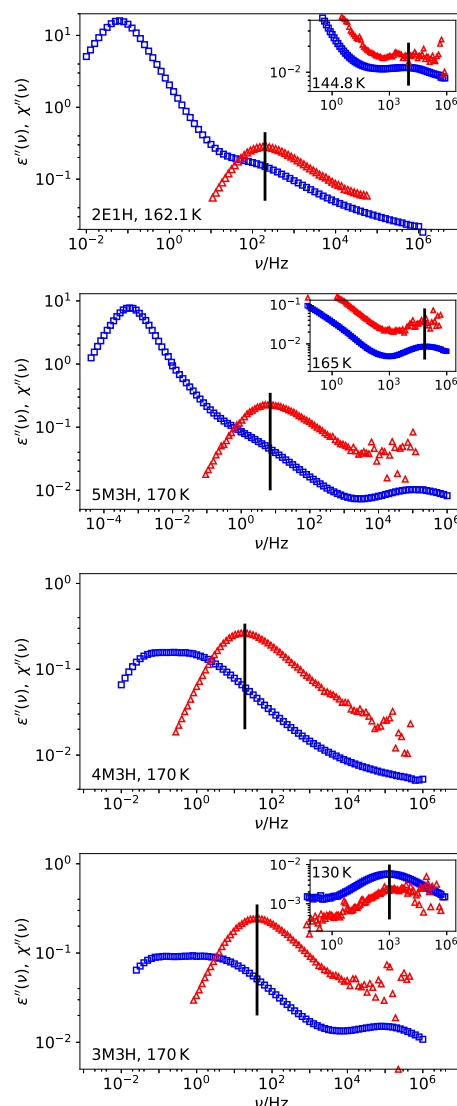


**FIG. 3.**  $\epsilon''$  (blue) and  $\chi''$  (red) of all four octanol isomers at selected temperatures. The black solid lines indicate the peak maximum frequency of  $\chi''$ . The insets display a comparison of the secondary relaxation processes between both techniques.

are identical and, thus,  $\chi''$  can be used to describe the self-part of dipolar relaxation.

We test this model for octanol isomers by attempting to fit  $\epsilon''$  using Eq. (3). For this purpose, we first fit  $\chi''$  using a generalized gamma distribution of relaxation times<sup>45</sup> with parameters  $\alpha = 2.0$  and  $\beta = 0.5$ , which are the same parameters as found for the generic shape of the  $\alpha$ -process identified in Ref. 35 and included in Fig. 2. Subsequently, the low-frequency part of  $\epsilon''$  is fitted by the Fourier transform of the Kohlrausch–William–Watts (KWW) function to describe the Debye process. The KWW function is chosen instead of the Debye function to take account of deviations from a pure Debye shape. For 2E1H and 5M3H, almost a pure Debye shape with

$0.98 < \beta < 1.0$  is found. In the ring-forming MAs 4M3H and 3M3H, the slow cross-correlation contribution is comparably weak, and its shape cannot be determined exactly. However, some broadening ( $\beta < 1$ ) is expected, considering that the Debye-like contribution is only weakly separated from the  $\alpha$ -process. We chose  $\beta = 0.65$ ; however, qualitatively similar results are obtained for different values of  $\beta$ . Finally, the parameter  $\Delta\varepsilon_\alpha$  is determined such that  $\varepsilon''$  is well-described at high-frequencies. The resulting fits are presented in Fig. 4 as black lines. Red symbols represent  $\Delta\varepsilon_\alpha \cdot \chi''(\nu)$  to illustrate its contribution to the entire fit function. Looking at Fig. 4, we observe that Eq. (3) is insufficient to describe  $\varepsilon''$  in the intermediate region between the Debye- and  $\alpha$ -processes, where the fit underestimates the intensity of the dielectric loss. We quantify the residual intensity by subtracting the fit function from  $\varepsilon''$ , and the results are included in Fig. 4 as the open black symbols. The relaxation strength of this missing contribution, which is not considered in Eq. (3), is similar to or even larger than the contribution on the time scale of the PCS  $\alpha$ -process for all octanol isomers. We show in the Appendix that qualitatively the same results are obtained when considering the PCS process to be slower by a potential factor of three, which could result from the difference in the Legendre polynomial. Moreover, it has to be noted that following the presented analysis, the respective relaxation strengths of the  $\beta$ -process in  $\varepsilon''$  and  $\chi''$  are different and has been adapted for during the fitting procedure. This finding stands in contrast to what have been found for short chain MAs, such as 1-propanol. Considering that the discrepancy regarding the aspects of molecular dynamics probed by the two techniques increases with increasing chain length of the carbon backbone, this behavior may not come as a surprise.

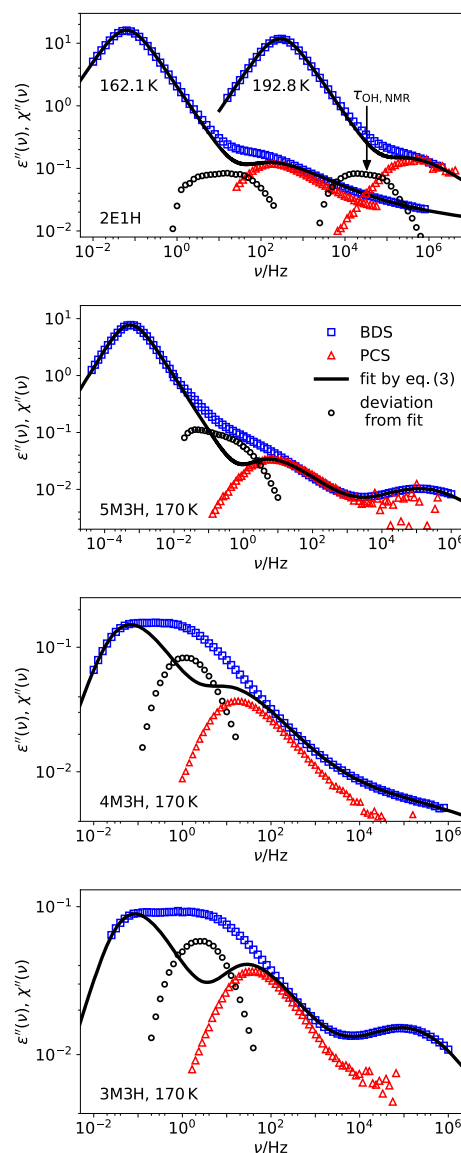
## DISCUSSION

As shown by the combined BDS and PCS data analysis in the previous section, the dielectric spectra of all investigated octanol isomers contain additional relaxation contributions in the intermediate region between the Debye process and the  $\alpha$ -process probed in PCS that reflect the reorientation dynamics of the entire molecule. A similar feature was found by Arrese-Igor *et al.*,<sup>29,30</sup> who identified an intermediate process in 2E1H and 5M3H via comparison to shear mechanical data.

To approach the question of how the intermediate process can be understood and, more generally, how the dielectric loss spectra of different MAs should be interpreted, we begin by analyzing the relaxation times of different processes and their temperature dependence in chain-forming MAs. Ring-forming MAs will be discussed at a later point.

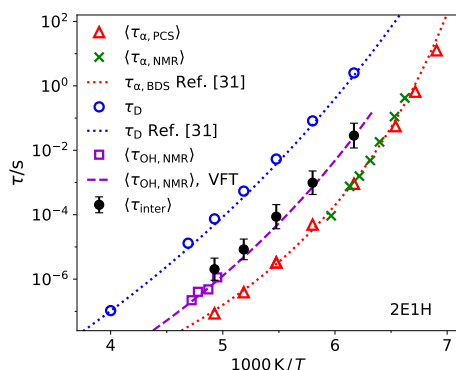
### Intermediate process in chain-forming MAs

Figure 5 shows the PCS and BDS relaxation times of 2E1H obtained from our combined analysis. In addition, NMR time constants determined from spin-lattice relaxation times of OD-deuterated 2E1H from Schildmann *et al.*,<sup>31</sup> ( $\tau_{\text{OH,NMR}}$ ) are included as purple symbols, and the Vogel-Fulcher-Tammann (VFT) fit to the NMR data is shown as the purple dashed line. Stimulated echo NMR time constants reflecting the  $\alpha$ -process are shown as green symbols and coincide with the PCS  $\alpha$ -process. To verify that sample temperatures between our experiments and the ones in



**FIG. 4.** Fit (black line) to the BDS data (blue) by Eq. (3) and PCS data (red), the amplitude of which was adapted in order to correspond to the contribution  $\Delta\varepsilon_{\alpha\beta} \cdot \chi''(\nu)$  to the BDS fit. In the intermediate region between the  $\alpha$ - and Debye-processes, Eq. (3) is insufficient to describe the data. This is illustrated by subtracting the fit from the BDS data (black symbols). For 2E1H, an additional higher temperature is included for which the NMR time constant ( $\tau_{\text{OH,NMR}}$ ) from Ref. 31 is indicated by the arrow.

Ref. 31 are comparable, we confirm that Vogel-Fulcher-Tammann (VFT) fits to the Debye- and alpha-process time-constants from the dielectric experiments performed in Ref. 31 (blue and red dotted lines) corresponds to our own data (symbols). To avoid systematic deviations between relaxation times due to differences in the applied model functions, mean relaxation times ( $\langle\tau\rangle$ ) are considered for our own and the NMR data, which are defined from the respective underlying distribution of relaxation times. Additionally, we



**FIG. 5.** Mean relaxation times of 2E1H from different techniques:  $\alpha$ -process time constants probed in PCS:  $\langle\tau_{\alpha,PCS}\rangle$ ; and NMR stimulated echos:  $\langle\tau_{\alpha,NMR}\rangle$ ; and determined from fits to BDS in Ref. 31,  $\tau_{\alpha,BDS}$ . Debye processes time constants from our fits:  $\tau_D$ ; and from Ref. 31. Intermediate time constants determined from  $^2\text{H-NMR}$  spin-lattice relaxation times:  $\langle\tau_{OH,NMR}\rangle$  plus the respective VFT fit; and from our own analysis:  $\langle\tau_{inter}\rangle$ .

include time constants for the intermediate process ( $\tau_{inter}$ ) that were extracted from the dielectric spectra by determining the respective peak maximum of the missing contribution shown in Fig. 4(a). The uncertainty of  $\langle\tau_{inter}\rangle$  was determined carefully by examining how different choices of fit parameters could alter the result.

As evident in Fig. 5, the relaxation times of the intermediate process ( $\tau_{inter}$ ) agree well with the reorientation time of the O–D-bond ( $\tau_{OD}$ ) determined by  $^2\text{H-NMR}$ , which is also included in Fig. 4(a) as the black arrow. The agreement between both time constants suggests that the intermediate process in  $\epsilon''$  is the dipolar signature of the O–H reorientation. Similar conclusions have been drawn by Arrese-Igor *et al.*<sup>29</sup> by comparing results from shear mechanical measurements to NMR data.

To further interpret the combined results from BDS and PCS, it is inevitable to consider how those techniques differ regarding the sensitivity toward different moieties of the molecules. As discussed earlier, PCS probes the reorientation of the entire octanol molecule and, thus, is dominated by the long carbon backbone. In contrast, BDS is only sensitive to the reorientation of the C–O–H moiety; more precisely, the O–H and C–O bonds contribute almost equally. Therefore, if the reorientation of the two bonds decouples, one expects to observe contributions to the dielectric loss on two separate time scales. This seems to be the case in 2E1H: The O–H reorientation was found to proceed on the time scale of the intermediate process. Additionally, we observe contributions to the dielectric loss on the time scale of the PCS  $\alpha$ -process, reflecting mostly the carbon backbone dynamics, which we expect to originate from the reorientation of the C–O bond as it is positioned close to the carbon backbone.

To provide a picture of how the decoupling of C–O and O–H bond dynamics could possibly be understood, we present a highly simplified sketch in Fig. 6. We consider a 2E1H molecule that is H-bonded into a chain-like suprastructure. Due to the H-bonding, the O–H reorientation is hindered, and its orientation is fixed with respect to the suprastructure. By contrast, the carbon backbone is able to perform large angle reorientations, as evident from the fact that the  $\alpha$ -process observed in PCS (yellow color in Fig. 6) was

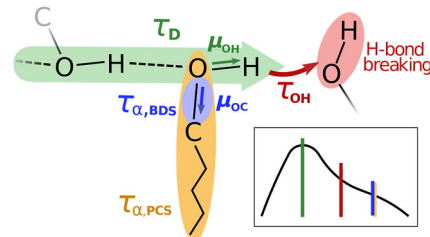


**FIG. 6.** Schematic illustration of the possible origin of different relaxation contributions in chain-forming MAs. The colors represent the different motional mechanisms probed by the different techniques. Yellow: Polarizability tensor probed by PCS; Blue: Dipole moment of the C–O bond; Red: Reorientation of the O–H bond due to breaking of H-bonds associated with the intermediate process; and Green: End-to-end dipole moment of suprastructure associated with the Debye process.

found to be significantly faster than O–H bond dynamics. While the dipole component  $\mu_{OH}$  is fixed with respect to the orientation of the suprastructure,  $\mu_{CO}$  is not fully restricted and, therefore, can rotate on a timescale  $\tau_{CO} \approx \tau_{\alpha,PCS}$  comparable to the rest of the carbon backbone (blue color). Its dielectric signature could be considered the dielectric  $\alpha$ -process, as it reflects the dynamics of the major part of the molecule. On the other hand, rotation of the O–H bond can only proceed if either the supramolecular chain structure rotates as a whole or if the molecule leaves the suprastructure. As  $\tau_{OH} < \tau_D$  is found, the latter mechanism seems predominant.<sup>9</sup> Consequently, the fact that the intermediate process, reflecting O–H bond reorientation, proceeds on time scales between the Debye- and  $\alpha$ -processes is a direct manifestation of the transient nature of the suprastructures in MAs.

For 5M3H, no detailed NMR results are available; however, the same interpretation is expected to be valid since the spectra shown in Figs. 3(b) and 4(b) correspond to comparably low temperatures where  $g_K > 1$  holds (cf. Fig. 1). Therefore, chain-like structures dominate, and a similar mechanism as in 2E1H is expected to occur. However, it is striking that the relaxation strength of the intermediate process is significantly stronger in 5M3H compared to 2E1H. An interpretation of this observation will be discussed below.

### Intermediate process in ring-forming MAs

Next, we consider the situation of the ring-forming octanol isomers 4M3H and 3M3H. For 4M3H, previous studies attempted to identify the dielectric  $\alpha$ -process via curve fits to the dielectric loss spectra.<sup>2,46,47</sup> As a result, they interpret the high-frequency maximum of the broad main peak to be the dielectric  $\alpha$ -process, superimposed by additional cross-correlation contributions at lower frequencies. By contrast, our PCS data provide a direct experimental pathway to identify the self-part of molecular reorientation dynamics, suggesting the  $\alpha$ -process to be significantly faster than the literature interpretation. Both interpretations are compared regarding their respective time-constants in Fig. 7, emphasizing the significant deviation of approximately one order of magnitude between  $\langle\tau_{\alpha,PCS}\rangle$  (red triangles) and the  $\alpha$ -process identified by Bauer *et al.*<sup>46</sup> from curve fits to the dielectric loss (dotted red line). We note that the deviation is significantly larger than a factor of three, which again could be due to the difference in the Legendre polynomial.<sup>36,48</sup>

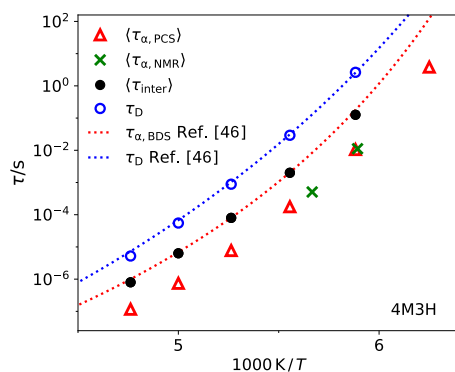


**FIG. 7.** Mean relaxation times of 4M3H from different techniques:  $\alpha$ -process time constants probed in PCS:  $\langle\tau_{\alpha,PCS}\rangle$ ; and NMR:  $\langle\tau_{\alpha,NMR}\rangle$ ; and determined from fits to BDS in Ref. 31,  $\tau_{\alpha,BDS}$ . Debye processes time constants from our fits:  $\tau_D$ ; and from Ref. 46. Intermediate time constants from our own analysis:  $\langle\tau_{inter}\rangle$ .

On the other hand, the relaxation times from NMR experiments  $\langle\tau_{\alpha,NMR}\rangle$ <sup>49</sup> (green symbols) coincide with  $\langle\tau_{\alpha,PCS}\rangle$ , supporting the findings from PCS. For 3M3H, similar results are obtained (not shown):  $\langle\tau_{\alpha,PCS}\rangle$  is faster than the prior dielectric interpretation of the  $\alpha$ -process, and an intermediate contribution is found following the analysis discussed above (see Fig. 4). Unfortunately, to our knowledge, no NMR results for 3M3H have been reported; however, we expect similar results to those found for 4M3H due to their similarity in most other respects.

Considering the results of the joint analysis of BDS and PCS data in Fig. 4, a pronounced dynamic decoupling of the carbon backbone and the O–H group is also observed for ring-forming MAs. Thus, the intermediate process in ring-forming MAs most likely reflects the characteristic time scale of molecules exiting ring structures.

### Intermediate process at elevated temperatures

Following our interpretation of the intermediate process, a necessary requirement for its appearance is the formation of H-bonded suprastructures that restrict the reorientation of O–H bonds and, thus, induce dynamic decoupling of different parts of the molecules. The number of molecules bound into different hydrogen-bonded states is temperature dependent, as was shown, e.g., by near-infrared (IR) spectroscopy measurements.<sup>2</sup> IR data for 4M3H from Bauer *et al.*<sup>50</sup> confirm this temperature dependence: While the number of unbonded hydroxy groups increases upon heating, the number of hydroxy groups that are included in a hydrogen-bonded structure decreases. Therefore, the contribution of both Debye- and intermediate processes to the dielectric loss spectrum should decrease upon heating until, at sufficiently high temperatures, all signatures of H-bonding disappear. Once this is the case, we do not expect to observe a dipolar cross-correlation contribution to the spectrum or any signature of dynamic decoupling between the carbon backbone and the C–O–H moiety of the molecules. As a consequence, no major difference should be observed between BDS and light-scattering spectra. In Fig. 8, we test this hypothesis by comparing the BDS and light-scattering spectra of 4M3H in the temperature

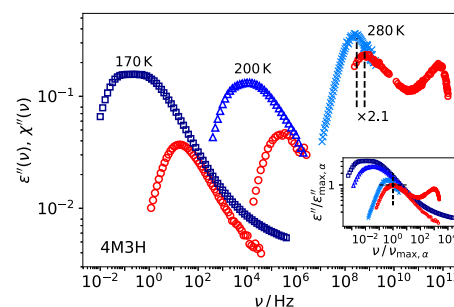


**FIG. 8.** Temperature evolution of  $\chi''$  (red symbols) and  $\epsilon''$  (blue symbols) of 4M3H from  $\sim T_g$  to the GHz regime. For  $\epsilon''$ , absolute amplitude values are shown, reflecting the significant temperature dependence of  $g_K$ ; cf. Fig. 1. The amplitude of  $\chi''$  is adjusted according to analyses, as shown in Fig. 4. In the inset,  $\chi''$  and  $\epsilon''$  are normalized to the peak maximum frequency and amplitude of the  $\alpha$ -process probed in light-scattering (red symbols).

range 170–280 K. The amplitudes of light-scattering data (red symbols) are adjusted to correspond to the  $\alpha$ -process contribution to the dielectric data (blue symbols) following analysis as shown in Fig. 4. While at low temperatures a distinct dynamic separation is observed between  $\chi''$  and  $\epsilon''$ , both quantities approach each other at high temperatures in the GHz regime. At 280 K,  $\chi''$  and  $\epsilon''$  have a very similar line shape and are separated by only a factor of  $\sim 2.1$ . These observations are highlighted in the inset of Fig. 8, where  $\chi''$  and  $\epsilon''$  are normalized to the respective peak maximum frequencies and amplitudes of  $\chi''$ . Indeed, we observe that with increasing temperature and, thus, decreasing H-bonding tendency, the difference between  $\chi''$  and  $\epsilon''$  vanishes.

### Relaxation strength of the intermediate process

Concerning the relative relaxation strength of the identified intermediate contributions to the dielectric loss, the applied fitting procedure gives an estimate to what degree molecular dynamics on the timescale of the PCS  $\alpha$ -process contribute to the dielectric loss, illustrated by the red symbols in Fig. 4. For tertiary octanol isomers (4M3H, 5M3H, and 3M3H), the latter contribution is of relatively low amplitude compared to the relaxation strength of the intermediate process. Therefore, we can conclude that the reorientation of the carbon backbone is weakly coupled to the reorientation of the molecular dipole moment in these MAs. The opposite is observed for the primary MA 2E1H, in harmony with the finding that a pronounced peak is observed in  $\epsilon''$  on the PCS  $\alpha$ -process time scale, while in all other octanol isomers, the peak maximum frequency of  $\chi''$  coincides with the high-frequency flank in  $\epsilon''$ .

In order to relate these differences to the molecular architecture, we consider in Fig. 9 single molecules of 2E1H and 4M3H, respectively, that are H-bonded into suprastructures. One notices that in both cases, in principle, a reorientation of the carbon backbone that leaves the dipole moment unaffected is possible in the form of a rotation around the C–O bond. In xM3H, such a reorientation, however, leads to more of a decorrelation of the carbon backbone than in 2E1H, as a consequence of the respective positions of the C–O–H moiety in the molecule (central vs terminal). Thus, if the backbone direction fully decorrelates, the dipole moment will

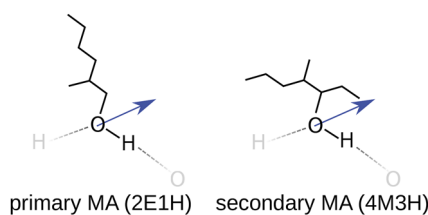


**FIG. 9.** Geometry of alcohol molecules bound into suprastructures via H-bonds for primary MAs such as 2E1H (left) and secondary MAs such as 4M3H (right). The molecular dipole moment is indicated by the blue arrow.

show a larger signature for primary MAs compared to tertiary MAs. Of course, this consideration is oversimplified as it ignores the internal degrees of freedom of the carbon-backbone itself, but still, it is a plausibility consideration showing why the carbon-backbone reorientation couples differently to the molecular dipole moment depending on the molecular architecture of MAs.

In addition to its relaxation strength, the spectral shape of the intermediate process is also found to vary among the different MAs. However, due to the indirect procedure of identifying the intermediate process, we refrain from interpreting its exact spectral shape. In order to do this in future studies, it would be beneficial to apply a more direct experimental approach, e.g., by utilizing triplet solvation dynamics. This technique resembles a local dielectric experiment by monitoring the dielectric response of a dye molecule's solvation shell and has recently been shown to be mostly insensitive toward dipolar cross-correlation in MAs.<sup>51</sup>

### Cross-correlation contributions to the dielectric loss

Due to the broad range of observed  $g_K$  values, the presented results for different octanol isomers allow a detailed analysis of the influence of dipolar cross-correlations on dielectric loss spectra. It is well established that dipolar cross-correlations are the origin of the low-frequency Debye process in MAs, while the self-part of dipolar relaxation is observed at higher frequencies. Naively assuming that the Debye process is the only contribution of dipolar cross-correlations to dielectric loss spectra, one obtains the relaxation strength of the self-part of dipolar dynamics as  $\Delta\epsilon_{\text{self}} = \Delta\epsilon - \Delta\epsilon_D$ . The intermediate process is explicitly included in the self-correlation part, as its origin is the dynamic decoupling of the dipole moment components  $\mu_{\text{OH}}$  and  $\mu_{\text{CO}}$ .

If the above assumption is justified, according to Onsager's equation,<sup>52</sup> different octanol isomers should have the same values of  $\Delta\epsilon_{\text{self}}$ , as they share the same dipole density. Figure 10 displays  $T \cdot \Delta\epsilon_{\text{self}}$  as a function of temperature for different octanol isomers, where the factor  $T$  eliminates the trivial Curie dependency of the overall relaxation strength. The large uncertainties reflect the fact that the choice of  $\beta$  [cf. Eq. (3)] strongly affects  $\Delta\epsilon_{\text{self}}$ . As evident from the figure,  $T \cdot \Delta\epsilon_{\text{self}}$  differs significantly between different octanol isomers. It is observed that  $T \cdot \Delta\epsilon_{\text{self}}$  follows the general trend of the respective Kirkwood factors  $g_K$  (2E1H > 5M3H > 4M3H  $\approx$  3M3H). Additionally, for 5M3H, the temperature dependence of  $g_K$  (cf. Fig. 1) is reflected in  $T \cdot \Delta\epsilon_{\text{self}}(T)$ . In the inset in Fig. 10, we plot  $\Delta\epsilon_{\text{self}}$  as a function of  $g_K$  for the different MAs. The factor  $T$  is

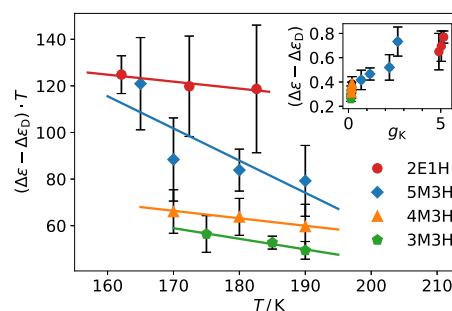


**FIG. 10.** Relaxation strength excluding the Debye process  $\Delta\epsilon - \Delta\epsilon_D$  multiplied by  $T$  to compensate for the trivial Curie temperature dependence. The solid lines represent linear fits to the data. The inset illustrates the correlation between  $\Delta\epsilon - \Delta\epsilon_D$  and  $g_K$ .

not included in this case, as it is already considered in  $g_K$ . The plot confirms the correlation between  $g_K$  and  $\Delta\epsilon_{\text{self}}$ .

The consequence of the presented correlation is that the Debye-like process is not the only manifestation of dipolar cross-correlations in the dielectric loss spectrum. Additionally, the self-part of dipolar relaxation seems to be weighted by a  $g_K$ -dependent factor. Similar conclusions were drawn in the early work of Williams *et al.*,<sup>53</sup> where, for a simple polymer model, dipolar cross-correlations were shown to only alter the amplitude of the self-correlations in the spectrum. We conclude that, in reality, dipolar cross-correlations seem to affect dielectric loss spectra in two ways: First, they usually lead to an additional contribution on slower time scales than the  $\alpha$ -process, i.e., the Debye process. Second, they apparently act as a weighting-factor for the self-part of the dielectric relaxation spectrum. These findings imply that the relation between  $\Delta\epsilon_D/\Delta\epsilon_\alpha$  and the average length  $N$  of chain-like structures, established in line with the transient chain model,<sup>9</sup> may be questioned, as the relation is based on the assumption that  $\Delta\epsilon_\alpha$  is unaffected by dipolar cross-correlations.

### CONCLUSION

From PCS measurements of four octanol isomers, we were able to determine relaxation times and the spectral shape of the  $\alpha$ -process. Despite the remarkable differences regarding the respective geometry of the predominantly formed suprastructures, the spectral shape probed in PCS coincides for all investigated MAs and agrees well with the recently proposed generic shape of the  $\alpha$ -process.<sup>35</sup> Via comparison to the PCS results, it was shown that the dielectric loss contains an additional intermediate relaxation contribution located in between the  $\alpha$ - and Debye processes for all octanol isomers, in harmony with results for 2E1H and 5M3H recently reported by Arrese-Igor *et al.*<sup>29,30</sup> Comparison to NMR results revealed that the intermediate process can be attributed to the reorientation of the hydroxy group, which decouples from the reorientation of the carbon backbone and also of the dipolar component carried by the C–O bond.

In addition, we analyzed the dielectric relaxation strength excluding the Debye-process  $\Delta\epsilon - \Delta\epsilon_D$ , which can be interpreted as the strength of the self-part of dipolar reorientation. However, it turned out that dipolar cross-correlations do not only appear as an



additional slow Debye process but, at the same time, seem to scale the relaxation strength of the self-part of dipolar reorientation by a  $g_K$ -dependent factor.

Generally, suprastructures in octanol isomers cause non-isotropic dipolar reorientation and decoupling of the dynamics of different molecular moieties carrying the dipole moment. This leads to broader and more complex distributions of relaxation times in BDS compared to the simple  $\alpha$ -process found in PCS. Similar effects are expected to be relevant in all MAs, as hydrogen bonding can result in the dynamic decoupling of different dipole moment components. However, a distinct intermediate process is difficult to identify in most MAs due to the rather small separation of the  $\alpha$ - and Debye processes, which is particularly large in the investigated octanols.

## ACKNOWLEDGMENTS

The financial support provided by the Deutsche Forschungsgemeinschaft under Grant No. BL 1192/3 is gratefully acknowledged.

## AUTHOR DECLARATIONS

### Conflict of Interest

The authors have no conflicts to disclose.

### Author Contributions

T.B. and T.R. contributed equally to this work.

**Till Böhmer:** Conceptualization (equal); Formal analysis (equal); Investigation (equal); Supervision (equal); Writing – original draft (equal); Writing – review & editing (equal). **Timo Richter:** Formal analysis (lead); Investigation (equal); Writing – original draft (equal); Writing – review & editing (supporting). **Jan Philipp Gabriel:** Conceptualization (equal); Investigation (supporting); Writing – review & editing (supporting). **Rolf Zeißler:** Formal analysis (equal); Investigation (equal); Writing – review & editing (equal). **Peter Weigl:** Conceptualization (equal); Writing – review & editing (equal). **Florian Pabst:** Investigation (equal); Supervision (equal); Writing – review & editing (equal). **Thomas Blochowicz:** Conceptualization (equal); Funding acquisition (equal); Project administration (equal); Resources (equal); Supervision (equal); Writing – review & editing (equal).

## DATA AVAILABILITY

The data that support the findings of this study are available from the corresponding author upon reasonable request.

## APPENDIX: CONSIDERING THE POTENTIAL FACTOR OF THREE

As discussed earlier, the reorientational relaxation times found in PCS could theoretically be up to a factor of three faster than the ones found in BDS just due to the different Legendre polynomials that are probed. While no conclusive evidence for a factor of three has been found for supercooled liquids, it is reason-

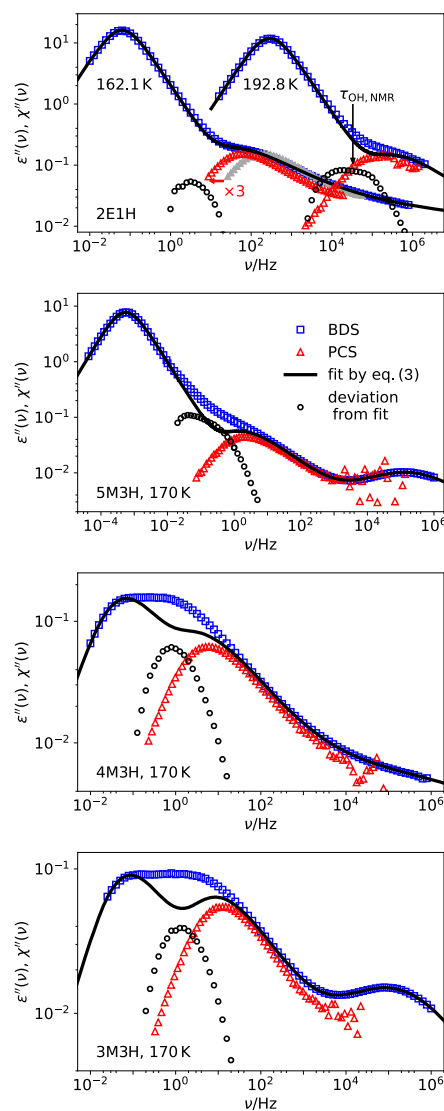


**FIG. 11.** Same analysis as shown in Fig. 4, with  $\chi''$  being shifted by a factor of three to lower frequencies to account for potential differences between the two techniques due to the different Legendre polynomials that are probed. The shift is indicated in the upper panel, where both the original data (gray) and the shifted data (red) are included.

able to consider how the results of the fitting procedure would be altered in the case that, indeed, the dielectric  $\alpha$ -process was slower by a factor of three. In Fig. 11, we performed the same analysis as shown in Fig. 4, with  $\chi''$  being shifted to lower frequencies by a factor of three. While the relaxation strength of the missing contribution decreases, the conclusions qualitatively remain unchanged: Eq. (3) is insufficient to describe  $\epsilon''$ , and we find an additional contribution to  $\epsilon''$  in between the Debye- and  $\alpha$ -processes.

## REFERENCES

- <sup>1</sup>R. H. Cole and D. W. Davidson, "High frequency dispersion in *n*-propanol," *J. Chem. Phys.* **20**, 1389–1391 (1952).
- <sup>2</sup>R. Böhmer, C. Gainaru, and R. Richert, "Structure and dynamics of monohydroxy alcohols—Milestones towards their microscopic understanding, 100 years after Debye," *Phys. Rep.* **545**, 125–195 (2014).
- <sup>3</sup>F. X. Hassion and R. H. Cole, "Dielectric relaxation processes in ethanol," *Nature* **172**, 212–213 (1953).
- <sup>4</sup>R. Minami, K. Itoh, H. Sato, H. Takahashi, and K. Higasi, "A theoretical approach to the dielectric relaxation of alcohol solutions," *Bull. Chem. Soc. Jpn.* **54**, 1320–1323 (1981).
- <sup>5</sup>Y. F. V. Levin and Y. D. Feldman, "Dipole relaxation in normal aliphatic alcohols," *Chem. Phys. Lett.* **87**, 162–164 (1982).
- <sup>6</sup>O. E. Kalinovskaya and J. K. Vij, "The exponential dielectric relaxation dynamics in a secondary alcohol's supercooled liquid and glassy states," *J. Chem. Phys.* **112**, 3262–3266 (2000).
- <sup>7</sup>U. Kaatz, R. Behrends, and R. Pottel, "Hydrogen network fluctuations and dielectric spectrometry of liquids," *J. Non-Cryst. Solids* **305**, 19–28 (2002).
- <sup>8</sup>D. Fragiadakis, C. M. Roland, and R. Casalini, "Insights on the origin of the Debye process in monoalcohols from dielectric spectroscopy under extreme pressure conditions," *J. Chem. Phys.* **132**, 144505 (2010).
- <sup>9</sup>C. Gainaru, R. Meier, S. Schildmann, C. Lederle, W. Hiller, E. Rössler, and R. Böhmer, "Nuclear-magnetic-resonance measurements reveal the origin of the Debye process in monohydroxy alcohols," *Phys. Rev. Lett.* **105**, 258303 (2010).
- <sup>10</sup>S. Stephenson, R. Offeman, G. Robertson, and W. Orts, "Hydrogen-bond networks in linear, branched and tertiary alcohols," *Chem. Eng. Sci.* **62**, 3019–3031 (2007).
- <sup>11</sup>M. Tomšič, A. Jamnik, G. Fritz-Popovski, O. Glatter, and L. Vlček, "Structural properties of pure simple alcohols from ethanol, propanol, butanol, pentanol, to hexanol: Comparing Monte Carlo simulations with experimental SAXS data," *J. Phys. Chem. B* **111**, 1738–1751 (2007).
- <sup>12</sup>P. Sillrén, J. Bielecki, J. Mattsson, L. Börjesson, and A. Matic, "A statistical model of hydrogen bond networks in liquid alcohols," *J. Chem. Phys.* **136**, 094514 (2012).
- <sup>13</sup>F. Palombo, P. Sassi, M. Paolantoni, A. Morresi, and R. S. Cataliotti, "Comparison of hydrogen bonding in 1-octanol and 2-octanol as probed by spectroscopic techniques," *J. Phys. Chem. B* **110**, 18017–18025 (2006).
- <sup>14</sup>J. L. MacCallum and D. P. Tieleman, "Structures of neat and hydrated 1-octanol from computer simulations," *J. Am. Chem. Soc.* **124**, 15085–15093 (2002).
- <sup>15</sup>G. Johari and W. Dannhauser, "Dielectric study of intermolecular association in sterically hindered octanol isomers," *J. Phys. Chem.* **72**, 3273–3276 (1968).
- <sup>16</sup>W. Dannhauser, "Dielectric study of intermolecular association in isomeric octyl alcohols," *J. Chem. Phys.* **48**, 1911–1917 (1968).
- <sup>17</sup>W. Dannhauser, "Dielectric relaxation in isomeric octyl alcohols," *J. Chem. Phys.* **48**, 1918–1923 (1968).
- <sup>18</sup>G. Johari and W. Dannhauser, "Evidence for structural transformation in liquid octyl alcohols from PVT studies," *J. Chem. Phys.* **48**, 3407–3408 (1968).
- <sup>19</sup>G. P. Johari and W. Dannhauser, "Viscosity of isomeric octyl alcohols as a function of temperature and pressure," *J. Chem. Phys.* **51**, 1626–1631 (1969).
- <sup>20</sup>C. Dugue, J. Emery, and R. A. Pethrick, "Ultrasonic and <sup>13</sup>C N.M.R. studies of isomeric octanols," *Mol. Phys.* **41**, 703–713 (1980).
- <sup>21</sup>L. Singh and R. Richert, "Watching hydrogen-bonded structures in an alcohol convert from rings to chains," *Phys. Rev. Lett.* **109**, 167802 (2012).
- <sup>22</sup>L. P. Singh, C. Alba-Simionesco, and R. Richert, "Dynamics of glass-forming liquids. XVII. Dielectric relaxation and intermolecular association in a series of isomeric octyl alcohols," *J. Chem. Phys.* **139**, 144503 (2013).
- <sup>23</sup>T. Hecksher and B. Jakobsen, "Communication: Supramolecular structures in monohydroxy alcohols: Insights from shear-mechanical studies of a systematic series of octanol structural isomers," *J. Chem. Phys.* **141**, 101104 (2014).
- <sup>24</sup>M. Becher, A. Lichtinger, R. Minikejew, M. Vogel, and E. A. Rössler, "Nmr relaxometry accessing the relaxation spectrum in molecular glass formers," *Int. J. Mol. Sci.* **23**, 5118 (2022).
- <sup>25</sup>J. Kirkwood, "The dielectric polarization of polar liquids," *J. Chem. Phys.* **7**, 911 (1939).
- <sup>26</sup>H. Fröhlich, *Theory of Dielectrics* (Clarendon Press, Oxford, 1958).
- <sup>27</sup>C. Böttcher and P. Bordewijk, *Theory of Electric Polarization II: Dielectrics in Time-Dependent Fields* (Elsevier, Amsterdam; London; New York, 1978).
- <sup>28</sup>A. Young-Gonzales and R. Richert, "Field induced changes in the ring/chain equilibrium of hydrogen bonded structures: 5-methyl-3-heptanol," *J. Chem. Phys.* **145**, 074503 (2016).
- <sup>29</sup>S. Arrese-Igor, A. Alegría, and J. Colmenero, "Multimodal character of shear viscosity response in hydrogen bonded liquids," *Phys. Chem. Chem. Phys.* **20**, 27758–27765 (2018).
- <sup>30</sup>S. Arrese-Igor, A. Alegría, A. Arbe, and J. Colmenero, "Insights into the non-exponential behavior of the dielectric Debye-like relaxation in monoalcohols," *J. Mol. Liq.* **312**, 113441 (2020).
- <sup>31</sup>S. Schildmann, A. Reiser, R. Gainaru, C. Gainaru, and R. Böhmer, "Nuclear magnetic resonance and dielectric noise study of spectral densities and correlation functions in the glass forming monoalcohol 2-ethyl-1-hexanol," *J. Chem. Phys.* **135**, 174511 (2011).
- <sup>32</sup>J. Gabriel, F. Pabst, and T. Blochowicz, "Debye-process and  $\beta$ -relaxation in 1-propanol probed by dielectric spectroscopy and depolarized dynamic light scattering," *J. Phys. Chem. B* **121**, 8847 (2017).
- <sup>33</sup>T. Böhmer, J. Gabriel, T. Richter, F. Pabst, and T. Blochowicz, "Influence of molecular architecture on the dynamics of h-bonded supramolecular structures in phenyl-propanols," *J. Phys. Chem. B* **123**, 10959–10966 (2019).
- <sup>34</sup>J. Gabriel, F. Pabst, A. Helbling, T. Böhmer, and T. Blochowicz, "Nature of the Debye-process in monohydroxy alcohols: 5-methyl-2-hexanol investigated by depolarized light scattering and dielectric spectroscopy," *Phys. Rev. Lett.* **121**, 035501 (2018).
- <sup>35</sup>F. Pabst, J. Gabriel, T. Böhmer, P. Weigl, A. Helbling, T. Richter, P. Zourchang, T. Walther, and T. Blochowicz, "Generic structural relaxation in supercooled liquids," *J. Phys. Chem. Lett.* **12**, 3685–3690 (2021).
- <sup>36</sup>J. Gabriel, F. Pabst, A. Helbling, T. Böhmer, and T. Blochowicz, "Depolarized dynamic light scattering and dielectric spectroscopy: Two perspectives on molecular reorientation in supercooled liquids," in *The Scaling of Relaxation Processes* (Springer International Publishing, Cham, 2018), pp. 203–245.
- <sup>37</sup>G. Diezemann, H. Sillescu, G. Hinze, and R. Böhmer, "Rotational correlation functions and apparently enhanced translational diffusion in a free-energy landscape model for the  $\alpha$  relaxation in glass-forming liquids," *Phys. Rev. E* **57**, 4398–4410 (1998).
- <sup>38</sup>A. Rivera, T. Blochowicz, C. Gainaru, and E. Rössler, "Spectral response from modulus time domain data of disordered materials," *J. Appl. Phys.* **96**, 5607–5612 (2004).
- <sup>39</sup>F. Pabst, J. Gabriel, P. Weigl, and T. Blochowicz, "Molecular dynamics of supercooled ionic liquids studied by light scattering and dielectric spectroscopy," *Chem. Phys.* **494**, 103–110 (2017).
- <sup>40</sup>J. Gabriel, T. Blochowicz, and B. Stühn, "Compressed exponential decays in correlation experiments: The influence of temperature gradients and convection," *J. Chem. Phys.* **142**, 104902 (2015).
- <sup>41</sup>T. Blochowicz, E. Gouirand, S. Schramm, and B. Stühn, "Density and confinement effects of glass forming *m*-toluidine in nanoporous Vycor investigated by depolarized dynamic light scattering," *J. Chem. Phys.* **138**, 114501 (2013).
- <sup>42</sup>F. Kremer and A. Schönhals, *Broadband Dielectric Spectroscopy*, 1st ed. (Springer, 2002).
- <sup>43</sup>L. N. G. Filon, "On a quadrature formula for trigonometric integrals," *Proc. R. Soc. Edinburgh, Sect. B: Biol. Sci.* **49**, 38–47 (1929).
- <sup>44</sup>R. Zeifler, F. Pabst, T. Böhmer, and T. Blochowicz, "Influence of intramolecular dynamics on the relaxation spectra of simple liquids," *Phys. Chem. Chem. Phys.* **25**, 16380 (2023).
- <sup>45</sup>T. Blochowicz, C. Tschirwitz, S. Benkhof, and E. A. Rössler, "Susceptibility functions for slow relaxation processes in supercooled liquids and the search for universal relaxation patterns," *J. Chem. Phys.* **118**, 7544–7555 (2003).
- <sup>46</sup>S. Bauer, H. Wittkamp, S. Schildmann, M. Frey, W. Hiller, T. Hecksher, N. B. Olsen, C. Gainaru, and R. Böhmer, "Broadband dynamics in neat 4-methyl-3-heptanol and in mixtures with 2-ethyl-1-hexanol," *J. Chem. Phys.* **139**, 134503 (2013).
- <sup>47</sup>S. Pawlus, M. Wikarek, C. Gainaru, M. Paluch, and R. Böhmer, "How do high pressures change the Debye process of 4-methyl-3-heptanol?," *J. Chem. Phys.* **139**, 064501 (2013).

<sup>48</sup>B. Berne and R. Pecora, *Dynamic Light Scattering* (Wiley, New York, 1976).

<sup>49</sup>S. Bauer, "Assoziationsgleichgewichte und dynamische Prozesse in glasbildenden Debye-Flüssigkeiten," Ph.D. thesis, Technische Universität Dortmund, 2015.

<sup>50</sup>S. Bauer, K. Burlafinger, C. Gainaru, P. Lunkenheimer, W. Hiller, A. Loidl, and R. Böhmer, "Debye relaxation and 250 K anomaly in glass forming monohydroxy alcohols," *J. Chem. Phys.* **138**, 094505 (2013).

<sup>51</sup>P. Weigl, D. Koestel, F. Pabst, J. P. Gabriel, T. Walther, and T. Blochowicz, "Local dielectric response in 1-propanol:  $\alpha$ -relaxation versus relaxation of mesoscale structures," *Phys. Chem. Chem. Phys.* **21**, 24778–24786 (2019).

<sup>52</sup>L. Onsager, "Electric moments of molecules in liquids," *J. Am. Chem. Soc.* **58**, 1486–1493 (1936).

<sup>53</sup>G. Williams, M. Cook, and P. J. Hains, "Molecular motion in amorphous polymers. consideration of the mechanism for  $\alpha$ ,  $\beta$  and ( $\alpha\beta$ ) dielectric relaxations," *J. Chem. Soc., Faraday Trans. 2* **68**, 1045–1050 (1972).